ESTIMATIVE OF INELASTICITY COEFFICIENT FROM EMULSION CHAMBER DATA

H M PORTELLA

Instituto de Física, Universidade Federal Fluminense, Av. Litorânea s/n, Gragoatá, 24210-340, Niterói, RJ, Brazil

L C S de OLIVEIRA and C E C LIMA

Centro Brasileiro de Pesquisas Físicas, Rua Dr. Xavier Sigaud 150, Urca, 22290-180, Rio de Janeiro, RJ, Brazil

Abstract

Atmospheric diffusion of high energy cosmic rays is studied analytically and the obtained integral electromagnetic fluxes are compared with the data measured by emulsion chamber detectors at mountain altitudes. We find a good consistency between them when the average nucleon inelasticity coefficient is varying between 0.50 and 0.65.

1 Introduction

The inelasticity is a global parameter of hadronic interactions and it is a crucial attribute in the calculation of the fluxes in cosmic ray cascades. It is defined as the fraction of energy giving up by the leading hadron in a collision induced by an incident hadron on a target nucleon or nucleus. The inelasticity, K_N, in a nucleon-induced interaction is related to the spectrum-weighted moments evaluated at $\gamma = 1$ (where γ is the power index of primary spectrum) as

$$1 - K_N = Z_{NN}(\gamma = 1) = \int_0^1 \eta \; f_{NN}(\eta) \; d\eta \quad .$$

Several authors have suggested that the average inelasticity-coefficient is an increasing function of the energy [1, 2], whereas others proposed that it is a decreasing function [3, 4, 5]. The behaviour of high energy cosmic rays, which reflects the nuclear interactions in the energy region $1 \sim 100$ TeV, indicates a constant value of the mean inelasticity equal to 0.50 [6]. A decreasing with energy of this parameter points out a strongly suppression of the pion production in this energy region and does not agree with cosmic ray observations.

The objective of this paper is to estimate the average inelasticity coefficient through the comparison of our calculations with the integral electromagnetic fluxes measured with large Emulsion Chamber Experiments at mountain altitudes. The main purpose is to describe in qualitative detail single events, *i.e.*, shower cores in their early stage of development observed at mountain altitudes.

Our calculation is performed by solving analitically the cosmic ray diffusion equations for electromagnetic showers in earth's atmosphere.

In these calculations we adopt to the particle production an approximated Feynman scaling in the fragmentation region. We have used the data on proton targets and on nuclear targets [7] to obtain the pion spectrum weighted moments. Although exist several functional forms to fit the behaviour of rising cross-section we assume the following one

$$\sigma = \sigma_0 \; (E/\epsilon)^{\alpha} \quad .$$

So, beginning with the measured all-particle primary spectrum we diffuse the particle showers down to the detection depths and we investigate our numerical results as a function of the adopted average inelasticity coefficient.

2 Hadronic and electromagnetic cascades in the Earth's atmosphere

The differential hadronic fluxes, $H(t,E)$ at a depth t in the energy range E and $E+dE$ are obtained integrating the nucleon and pion diffusion equations using the semigroup theory. We assume that only the pions are generated in the multiparticle production neglecting the particles with small fractions such as kaons, heavy mesons, etc.. In this case the solutions are [8];

$$N(t,E) = \sum_{n=0}^{\infty} \frac{(-1)^n}{n!} \left(\frac{t}{\lambda_N(E)}\right)^n \prod_{i=1}^{n} \left(1 - Z_{NN}(\gamma,\alpha,n)\right) N(0,E) \tag{1}$$

with

$$Z_{NN}(\gamma,\alpha) = \int_0^1 f_{NN}(\eta)\ \eta^{\gamma-i\alpha}\ d\eta \tag{2}$$

where η is the elasticity coefficient of the nucleons in the atmosphere that is distibuted according to $f_{NN}(\eta)$.

The pionic fluxes are

$$\Pi(t,E) = \sum_{m=0}^{\infty}\sum_{n=0}^{\infty} \int_0^t dz\ \frac{(-1)^m(-1)^n}{m!\ n!} \left(\frac{t-z}{\lambda_\pi(E)}\right)^m \left(\frac{z}{\lambda_N(E)}\right)^n Z_{N\pi}(\gamma,\alpha,n)\cdot$$

$$\cdot \prod_{i=1}^{n}\left(1 - Z_{NN}(\gamma,\alpha,n)\right) \prod_{j=1}^{m}\left(1 - Z_{\pi\pi}(\gamma,\alpha,m,n)\right) \frac{N(0,E)}{\lambda_N(E)} \tag{3}$$

with

$$Z_{\pi\pi}(\gamma,\alpha,m,n) = \int_0^1 f_{\pi\pi}(x)\ x^{\gamma-\alpha(j+n+1)}\ dx \tag{4}$$

and

$$Z_{N\pi}(\gamma,\alpha,n) = \int_0^1 f_{N\pi}(x)\ x^{\gamma-\alpha(n+1)}\ dx \quad . \tag{5}$$

The $f_{N\pi}(x)$ and $f_{\pi\pi}(x)$ are the energy spectra of the pions produced in the nucleon-air and in the pion-air interactions respectively, and x is the Feynman variable ($x = 2p_L/\sqrt{S}$).

The solutions (1) and (3) are subjected to the boundary conditions

$$N(0,E) = N_0\ E^{-(\gamma+1)} \tag{6}$$

and

$$\Pi(0,E) = 0 \tag{7}$$

that represents the nucleon and pion fluxes at the top of atmosphere.

The above solutions are obtained considering the interaction mean-free paths in the power form, $\lambda_{\ H}(E) = \lambda_{0_H}\ E^{-\alpha}$ ($_H = {}_N$ or π).

Using naive approximations [9] we can write the solutions (1) and (3) in the following forms

$$N(t,E) = N(0,E)\ e^{-t\,\omega_N(E)} \tag{8}$$

and

$$\Pi(t,E) = N(0,E)\frac{\omega_{N\pi}(\gamma,E)}{\omega_N(E) - \omega_\pi(E)} \left(e^{-t\,\omega_\pi(E)} - e^{-t\,\omega_N(E)}\right) \quad . \tag{9}$$

The $\omega_N(E)$, $\omega_\pi(E)$ and the $\omega_{N\pi}(\gamma,E)$ functions are described in the appendix A.

The production rate of γ-rays originated from the π^0 decay is given by [10]

$$P_\gamma(z,E_\gamma) = 2\int_{E_\gamma}^{\infty} \frac{dE'}{2E'} \left(P_{\pi^\pm}^{N-air} + P_{\pi^\pm}^{\pi^\pm-air}\right) \tag{10}$$

where $P_{\pi^\pm}^{N-air}$ and $P_{\pi^\pm}^{\pi^\pm-air}$ are the production rate of the charged pions from the nucleon-air and pion-air interactions and are represented by

$$P_{\pi^\pm}^{H-air} = \int_0^1 \frac{H(z,E_0)}{\lambda_H(E_0)}\, f_{H\pi}(x)\, \frac{dx}{x} \qquad ; \qquad {}_{H\,=\,N} \text{ or } \pi \quad . \tag{11}$$

In the expression (10) we have used that the secondary pions are formed with equal multiplicity, so the number of π^0 is half of the number of charged pions.

The differential flux of the electromagnetic component can be written as

$$F_{\gamma,e}(t,E) = \int_0^t dz \int_E^\infty dE_\gamma\; P_\gamma(z,E_\gamma)\; (e+\gamma)(t-z,E_\gamma,E) \tag{12}$$

where $(e+\gamma)(t-z,E_\gamma,E)$ are the photons, electrons and positrons produced by a single photon. They are computed using the approximation **A** [11] and are written in the following form

$$(e+\gamma)(t-z,E_\gamma,E) = \frac{1}{2\pi i}\int_C \left(\frac{E_\gamma}{E}\right)^s \frac{1}{E}\left(N_1(s)e^{\lambda_1(s)(t-z)/X_0} + N_2(s)e^{\lambda_2(s)(t-z)/X_0}\right) \quad . \tag{13}$$

The functions $N_i(s)$, $\lambda_i(s)$ and X_0 are the parameters with standardized definitions in cascade theory [11]. These functions and the evaluation of the electromagnetic fluxes are presented in the appendix B.

In order to compare our calculations for electromagnetic showers with the emulsion chamber data measured at mountain altitudes we need to obtain the integral fluxes of this component. They are,

$$F_{\gamma,e}(t,\geq E) = \int_E^\infty F_{\gamma,e}(t,E)\; dE \tag{14}$$

3 Comparison with experimental data

Emulsion Chamber Experiments at mountain altitudes are very simple detectors constituted of multiple sandwich of material layers (Pb, Fe, etc.) and photo-sensitive layers (X-ray films, nuclear emulsions plates, etc.). They can detect electromagnetic showers of high energy ($E_{e,\gamma} \geq$ 1 TeV) and due to its powerful spatial resolution and energy determination they can study in details the cosmic-ray interactions.

The experimental data are taken from J. R. Ren *et al.* [19] for Mt. Kanbala; C. M. G. Lattes *et al.* [13] for Mt. Chacaltaya and M. Amenomori *et al.* [21] for Mt. Fuji.

The experimental fluxes at Mt. Chacaltaya are revised according to the energy determination introduced by M. Okamoto and T. Shibata [22] where the LPM and spacing effects were taken into account. This revision followed the same procedure made by N.M. Amato and N. Arata [20] for determination of total hadron fluxes.

In order to make a comparison with electromagnetic fluxes measured with these detectors it is necessary to check the main assumptions made in our calculations;

a) Primary cosmic-ray radiation

The energy spectra obtained by Emulsion Chamber Experiments at mountain altitude are in the region of $3 \sim 50$ TeV for (e,γ) component and $3 \sim 40$ TeV for hadronic shower. So, we need to include in our calculations the primary spectrum up to knee ($\approx 10^{15}$ eV). In the present work we assume the primary cosmic-ray radiation in integral form reported by J. Bellandi Filho *et al.* [14] from JACEE data [15].

$$N_1(0,\geq E) = 1.12\cdot 10^{-6}(E/5\text{TeV})^{-1.7}(/\text{cm}^2.\text{s.st}) \tag{15}$$

where E(TeV/nucleus).

Nucleonic intensity at $t=0$, equivalent to primary cosmic-ray radiation is given by

$$N(0,\geq E) = A^{1-\gamma} N_1(0,\geq E) \tag{16}$$

where A is the average mass number of cosmic ray nuclei; we adopt $A = 14.0$ which is the value in low energy region (E/part $< 10^{14}$ eV).

b) Collision mean free paths

We use to fit the behaviour of rising with energy of the p-air inelastic cross-section the following form [7, 14, 16, 17],

$$\sigma_N(E) = \sigma_{N_0}(E/\mathrm{TeV})^{\alpha} \tag{17}$$

with $\sigma_{N_0} = 300$ mb and $\alpha = 0.06$ [7, 14].

So, the collision mean free path of the nucleon in the earth's atmosphere is expressed by

$$\lambda_N(E) = \lambda_{N_0}(E/\mathrm{TeV})^{-\alpha} \tag{18}$$

with $\lambda_{N_0} = 80$ g/cm^2 [7, 14].

For the pion mean free paths we assume that $\lambda_{\pi_0}/\lambda_{N_0} \approx 1.4$ and that they have the same energy dependence, like in the nucleon case [14]. Thus, we have

$$\lambda_\pi(E) = \lambda_{\pi_0}(E/\mathrm{TeV})^{-\alpha} \tag{19}$$

with $\lambda_{\pi_0} = 112$ g/cm^2.

c) Secondary pions:

The functions $f_{N\pi}(x)$ and $f_{\pi\pi}(x)$ are the energy distribution of secondary nucleons and pions for nucleon-air and pion-air interactions, respectively. We have used in this calculation the data on proton targets and on nuclear targets [7] to obtain these functions and they are written as

$$f_{N\pi}(x) = 2.08\ \frac{(1-x)}{x}\ e^{-5x} \tag{20}$$

and

$$f_{\pi\pi}(x) = \frac{2.6}{x}\left(1 + \frac{x}{0.45}\right)^{-3} + \frac{0.32}{x}\ e^{2(x-1)} \tag{21}$$

these functions are for two charged states of pions and the contribution of leading pions are taken into account in the last one.

Figures 1-3 show the comparison of our solution with the integral electromagnetic fluxes measured at Mt. Kanbala (520 g/cm^2), Mt. Chacaltaya (540 g/cm^2) and Mt. Fuji (650 g/cm^2), respectively. Two curves are also drawn in the figures for $< K_N > = 0.50$ and 0.65, taking into account the above mentionated itens.

4 Conclusions

We have solved the diffusion equations of cosmic-ray hadrons analytically and after this we derived the integral electromagnetic fluxes using the approximation **A** of the electromagnetic cascade theory.

These fluxes at mountain atmospheric depths decrease when we include in our calculation the rising of the cross-section and the decreasing of the mean nucleon elasticity.

We conclude that the naive assumptions for the secondary production based on approximate scaling in the fragmentation region is possible to explain experimental data on integral electromagnetic fluxes detected in large emulsion chamber experiments.

This scenario requires a mean nucleon inelasticity coefficient varying from 0.50 to 0.65. At low energy (few TeV) the agreement between experimental data and the calculated fluxes shows that $< K_N > \approx 0.50$, that is the adjust indicated by former workers in the cosmic ray literature. For $E > 10$ TeV we see from the figure that $< K_N > \approx 0.65$. Therefore, with this simple analysis we see that the nucleon inelasticity coefficient appears to show a tendency of rising with energy according to Mini-jet Models [17] and Quark-Gluon String Models [2]. These integral fluxes are somewhat affected when the coefficient α changes in the interval 0.06 to

0.10, which is the appropriated values to explain the experimental data for mountain emulsion chambers experiments. In the latter the fit between our calculation and the experimental data is obtained for $< K_N >$ changing between approximately 0.45 and 0.60.

These results are in agreement with that of L. Jones [18] based in an analysis on inclusive reactions data from accelerator, with analytical calculations on nucleon fluxes at sea level [9] and with hadron and electromagnetic fluxes at mountain altitudes [8, 10].

Appendix A

Hadronic cascades

The functions $\omega_N(E)$, $\omega_\pi(E)$ and $Z_{N\pi}(\gamma, E)$ in the hadronic fluxes (8) and (9) are [9]

$$\omega_N(E) = \omega_N \; E^{0.06} = \frac{1}{\lambda_N(E)} \left(1 - \frac{1}{2} Z_{NN}(\gamma) - \frac{1}{2} Z_{NN}(\gamma, \alpha)\right) \tag{22}$$

$$\omega_\pi(E) = \omega_\pi \; E^{0.06} = \frac{1}{\lambda_\pi(E)} \left(1 + \frac{1}{2} Z_{\pi\pi}(\gamma) - \frac{3}{2} Z_{\pi\pi}(\gamma, \alpha)\right) \tag{23}$$

and

$$\omega_{N\pi}(E) = \frac{Z_{N\pi}(\gamma, \alpha)}{\lambda_N(E)} = \frac{1}{\lambda_N(E)} \int_0^1 x^{\gamma-\alpha} \; f_{N\pi}(x) \; dx \tag{24}$$

where

$$Z_{NN}(\gamma, \alpha) = \int_0^1 \eta^{\gamma-\alpha} \; f_{NN}(\eta) \; d\eta \tag{25}$$

and

$$Z_{\pi\pi}(\gamma, \alpha) = \int_0^1 x^{\gamma-\alpha} \; f_{\pi\pi}(x) \; dx \quad . \tag{26}$$

The functions $f_{N\pi}(x)$ and $f_{\pi\pi}(x)$ are the energy distribution of secondary nucleons and pions for nucleon-air and pion-air interactions, respectively (see item c of section 3).

The nucleon elasticity distribution is assumed to be [9]

$$f_{NN}(\eta) = (1 + \beta)(1 - \eta)^\beta \tag{27}$$

where $\eta = E/E'$ and β fulfills a consistency relation between the mean elasticity and average inelasticity, so that $< N > + < K > = 1$, for nucleons. When $\beta = 0$ we have the nucleon uniform distribution of elasticity ($< \eta > = 0.5$).

Appendix B

Electromagnetic cascades

The production rate of γ-rays produced from π^0 decay expression (10) can be written as

$$P_\gamma(z, E_\gamma) = \frac{N_0 \; E_\gamma^{-(\gamma+1-\alpha+z\,\alpha\,\omega_N)} e^{-z\,\omega_N}}{\gamma + 1 - \alpha + z\;\alpha\;\omega_N} \left(\frac{Z_{N\pi}(\gamma - \alpha + z\;\alpha\;\omega_N)}{\lambda_{N_0}} - \frac{Z_{\pi\pi}(\gamma - \alpha + z\;\alpha\;\omega_N)}{\lambda_{\pi^0}} \right.$$

$$\left. \frac{\omega_{N\pi}(E)}{\omega_N(E) - \omega_\pi(E)} \right) + \frac{N_0 E^{-(\gamma+1-\alpha+z\,\alpha\,\omega_\pi)}}{(\gamma + 1 - \alpha + z\;\alpha\;\omega_\pi)} \frac{\omega_{N\pi}(E) e^{-z\,\omega_\pi}}{(\omega_N(E) - \omega_\pi(E))} \frac{Z_{\pi\pi}(\gamma - \alpha + z\;\alpha\;\omega_\pi)}{\lambda_{\pi^0}} \quad . \tag{28}$$

The Z-factors $Z_{N\pi}$ and $Z_{\pi\pi}$ is the last expression are

$$Z_{N\pi}(\gamma - \alpha + z\;\alpha\;\omega_N) = \int_0^1 x^{\gamma-\alpha+z\,\alpha\,\omega_N} \; f_{N\pi}(x) dx \tag{29}$$

and

$$Z_{\pi\pi}(\gamma - \alpha + z\ \alpha\ \omega_i) = \int_0^1 x^{\gamma-\alpha+z\,\alpha\,\omega_i}\ f_{\pi\pi}(x)\ dx \quad i = N \text{ or } \pi\ . \tag{30}$$

The expression (28) was obtained considering the expansion

$$\frac{1}{\lambda_{\rm H}(E)} = \frac{1 + \alpha\ ln(E/E_0)}{\lambda_{0_{\rm H}}} \qquad ; \qquad H = N \text{ or } \pi \tag{31}$$

The differential flux of the electromagnetic component (12) is obtained from this production rate and evaluated at the poles $s_1 = \gamma - \alpha + z\ \alpha\ \omega_N$ and $s_2 = \gamma - \alpha + z\ \alpha\ \omega_\pi$.

The integral flux is put in the form

$$F_{\gamma,e}(t, \geq E) = F_{\gamma_1,e}(t, \geq E) + F_{\gamma_2,e}(t, \geq E) \tag{32}$$

with

$$F_{\gamma_1,e}(t, \geq E) = \int_0^t dz\ \frac{N_0\ E^{-s_1}\ e^{-z\,\omega_N}}{s_1(s_1+1)} \left(N_1(s_1)e^{\lambda_1(s_1)(t-z)/X_0} + N_2(s_1)e^{\lambda_2(s_1)(t-z)/X_0}\right) C_1(s_1) \tag{33}$$

and

$$F_{\gamma_2,e}(t, \geq E) = \int_0^t dz\ \frac{N_0\ E^{-s_2}\ e^{-z\,\omega_\pi}}{s_2(s_2+1)} \left(N_1(s_2)e^{\lambda_1(s_2)(t-z)/X_0} + N_2(s_2)e^{\lambda_2(s_2)(t-z)/X_0}\right) C_2(s_2) \tag{34}$$

where

$$C_1(s_1) = \frac{Z_{N\pi}(s_1)}{\lambda_{0_N}} - \frac{\omega_{N\pi}(E)}{(\omega_N(E) - \omega_\pi(E))}\frac{Z_{\pi\pi}(s_1)}{\lambda_{0_\pi}} \tag{35}$$

and

$$C_2(s_2) = \frac{\omega_{N\pi}(E)}{(\omega_N(E) - \omega_\pi(E))}\frac{Z_{\pi\pi}(s_2)}{\lambda_{0_\pi}} \tag{36}$$

with

$$Z_{N\pi}(s_i) = \int_0^1 x^{s_i}\ f_{N\pi}(x)\ dx \tag{37}$$

and

$$Z_{\pi\pi}(s_i) = \int_0^1 x^{s_i}\ f_{\pi\pi}(x)\ dx \quad . \tag{38}$$

The functions N_i and λ_i are the usual parameters with definitions in cascade theory and can be obtained in the reference [11]. X_0 is the radiation length in the atmosphere ($X_0 = 37.1$ g/cm^2).

References

[1] J. D. de Deus, *Phys. Rev.* **D32** (1985) 2334.

[2] A. B. Kaidalov and K. A. Ter-Martyrosian, *Phys. Lett.* **B117** (1982) 247;
A. B. Kaidalov and K. A. Ter-Martyrosian, *Sov. J, Nucl. Phys.* **40** (1984) 135.

[3] G. N. Fowler *et al.*, *Phys. Rev.* **D35** (1987) 870;
G. N. Fowler *et al.*, *Phys. Rev.* **C40** (1989) 1219.

[4] A. Ohsawa and K. Sawayanagi, *Phys. Rev.* **D49** (1992) 3128.

[5] Z. Wlodarczyk *et al.*, *J. Phys. G* **21** (1995) 281.

[6] C. R. A. Augusto *et al.*, *Phys. Rev.* **D61** (1999) 012003;
A. Ohsawa, *Prog. Theor. Phys.*, **92** (1994) 1005.

[7] H. M. Portella, *PhD Thesis* (CBPF: Centro Brasileiro de Pesquisas Físicas, Brazil), (1989).

[8] H. M. Portella, N. Amato, R. H. C. Maldonado and A. S. Gomes, *J. Phys. A: Math. Gen.* **31** (1998) 6861.

[9] J. Bellandi Filho *et al.*, *Il Nuovo Cimento* **A101** (1989) 897.

[10] H. M. Portella *et al.*, *ICRR-Report 454-99-12* Institute for Cosmic Ray Research, University of Tokyo (1999) 31.

[11] J. Nishimura, *Handbuch Der Physik* (Reading: Springer-Verlag) (1967) 1.

[12] M. Akashi *et al.*, *Il Nuovo Cimento* **A65** (1981) 355.

[13] C. M. G. Lattes *et al.*, *Proc. 13th Int. Symp. on Very High Energy Cosmic Ray Interactions* (Denver) **13** (1973) 2219.

[14] J. Bellandi Filho *et al.*, *Prog. Theor. Phys.* **83** (1990) 58.

[15] T. H. Burnett *et al.* (JACEE Collaboration), *Proc. of the Int. Symp. on Cosmic Ray and particle Physics* (ICRR, Univeristy of Tokyo) (1984) 468.

[16] B. Z. Kopeliovich *et al.*, *Phys.Rev.* **D39** (1989) 769.

[17] T. K. Gaisser, *Cosmic Ray and Particle Physics* (Cambridge: Cambridge University Press), (1990).

[18] L. W. Jones, *Proc. of 2th Int. Symp. on Very High Energy Cosmic Ray Interactions* (La Paz-Rio de Janeiro) (1982) 1.

[19] J. R. Ren *et al.*, *Nuovo Cimento* **10C** (1987) 43.

[20] N. M. Amato and N. Arata, *Proc. 5th Int. Symp. on Very High Energy Cosmic Ray Interactions* (Lodz) (1988) 49.

[21] M. Amenomori *et al.*, *Proc. 18th Int. Cosmic Ray Conf.* (Bangalore) **11** (1983) 57.

[22] M. Okamoto and T. Shibata, *Nucl. Inst. and Meth.* **A257** (1987) 155.

Figure Captions

Figure 1 - Integral electromagnetic spectrum at Mt. Kanbala (520 g/cm^2). The full lines represent the calculated flux for $< K_N >= 0.65$ and the dashed lines for $< K_N >= 0.50$. All lines are for $\alpha = 0.06$. The experimental data are taken from J. R. Ren *et al.* [19].

Figure 2 - Integral electromagnetic spectrum at Mt. Chacaltaya (540 g/cm^2). The full lines represent the calculated flux for $< K_N >= 0.65$ and the dashed lines for $< K_N >= 0.50$. All lines are for $\alpha = 0.06$. The experimental data are taken from C. M. G. Lattes *et al.*(black dots) [13].

Figure 3 - Integral electromagnetic spectrum at Mt. Fuji (650 g/cm^2). The full lines represent the calculated flux for $< K_N >= 0.65$ and the dashed lines for $< K_N >= 0.50$. All lines are for $\alpha = 0.06$. The experimental data are taken from M Amenomori *et al.* [21].

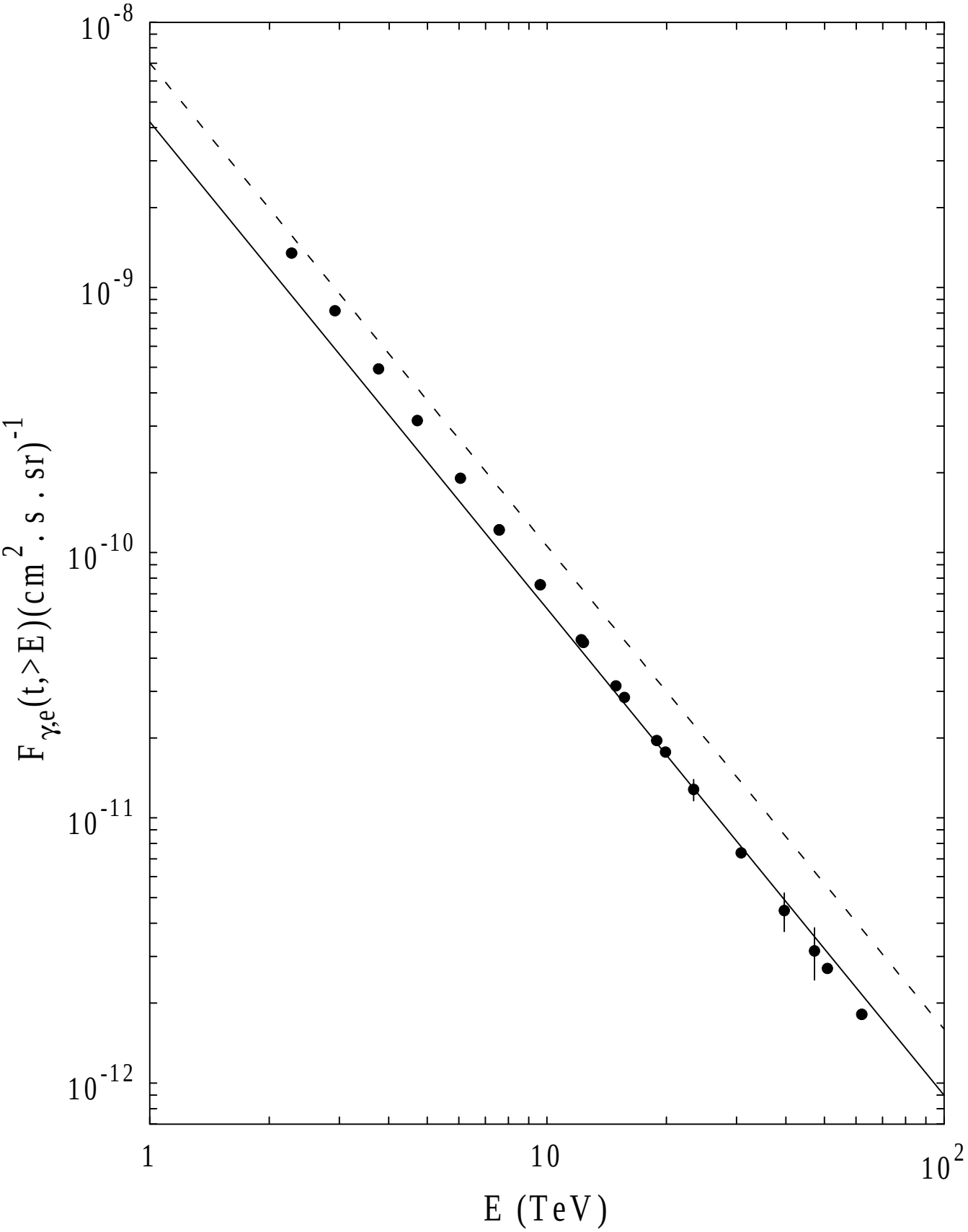

Figure 1

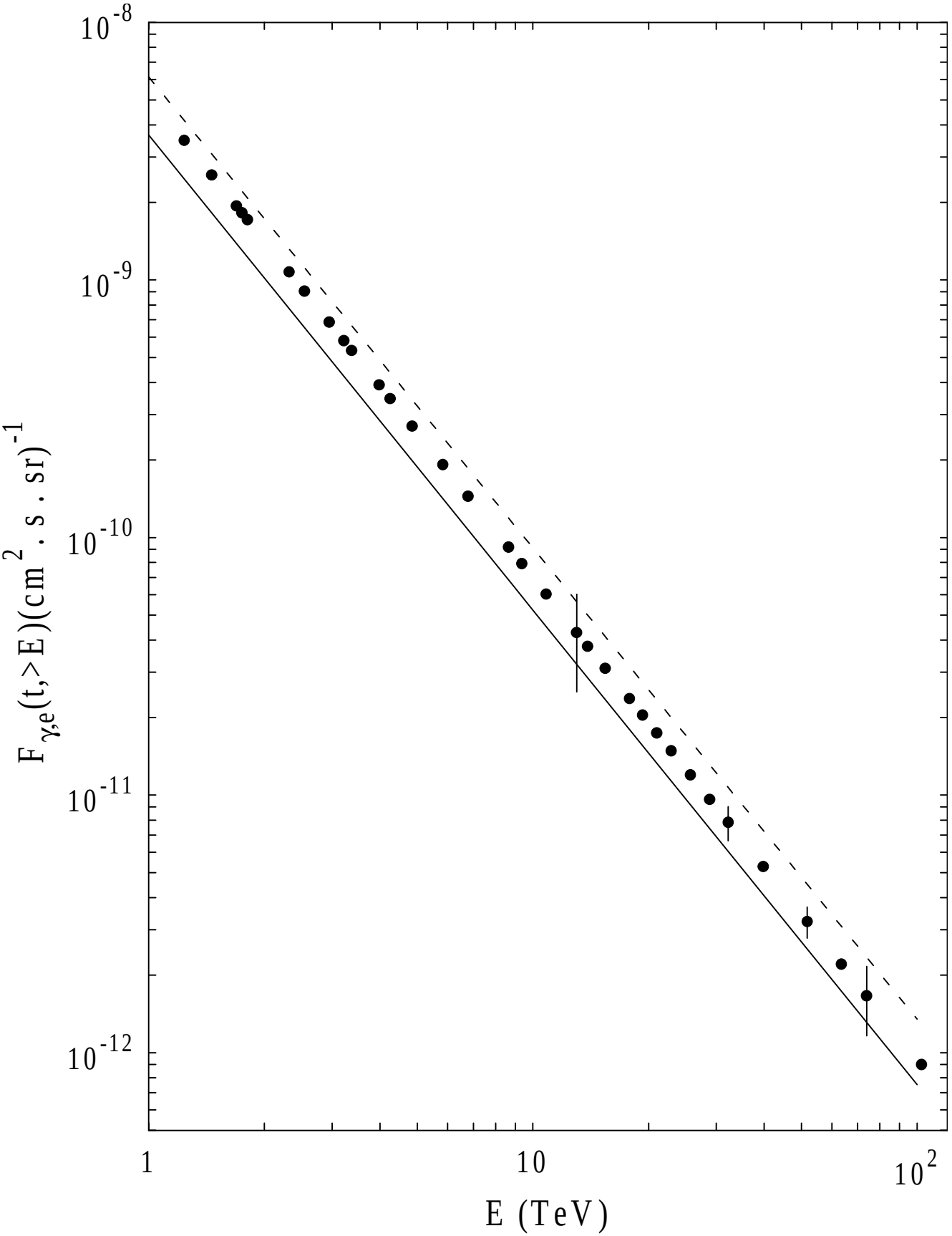
10^{-8}
10^{-9}
10^{-10}
10^{-11}
10^{-12}
$F_{\gamma,e}(t,>E)(cm^2 \cdot s \cdot sr)^{-1}$
1
10
10^2
E (TeV)

Figure 2

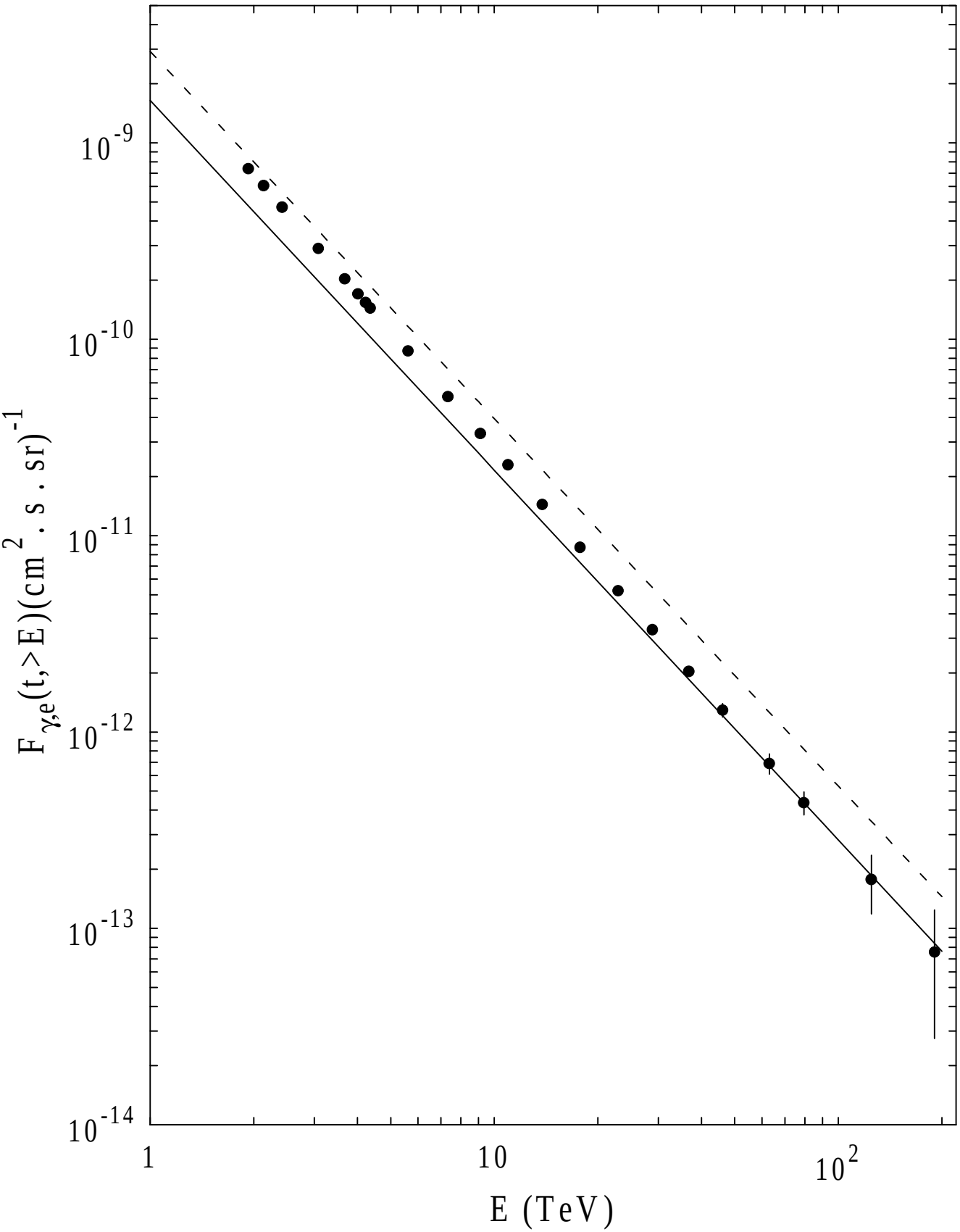

Figure 3